New Real Time UTC(CH) Generation Scheme at METAS: Recent Progress in Control and Calibration Methods

Laurent-Guy Bernier, Gregor Dudle and Christian Schlunegger
Swiss Federal Office of Metrology METAS
Lindenweg 50, CH-3003 Bern-Wabern, Switzerland
Email: laurent-guy.bernier@metas.ch

***Abstract*— In the course of the year 2007, UTC(CH) will change from a computed time scale definition to one based on a real-time master clock. In preparation for this important change, the time scale generation hardware was upgraded and new control software is being developed. This paper discusses recent progress in the development of control and calibration methods used in the new time scale generation system and reports experimental results obtained during validation testing.**

I. Introduction

UTC(CH) is different from many other UTC(k) in the sense that it is actually a *computed* time scale defined only for epoch UTC 00:00 of each day. UTC(CH) is generated as the weighted average of five free running atomic clocks and it is steered monthly to track UTC. However this is going to change. In 2006 we began to phase in a new system intended to supersede the original one. In the new time scale generation scheme UTC(CH) becomes a steered master clock. A description of the architecture of the upgraded system and a discussion of the advantages and disadvantages of a paper clock versus a master clock definition of UTC(CH) were reported at the last PTTI meeting [1]. The architecture of the new system is similar to time scale generation schemes used at USNO [2] and elsewhere in other NMIs [3]. The work that is still in progress now, *i.e.* control software development and validation testing, is the last phase of development before the new definition of UTC(CH) can be commissioned. The present paper discusses recent progress in the development of the control and calibration methods used in the time scale generation system and reports experimental results obtained during validation testing.

II. New Architecture

Figure 1 shows the new time scale generation scheme whereby UTC(CH) is defined as a hardware master clock. The definition of UTC(CH) via hardware eliminates the drawbacks of the paper clock definition. Measurements can be referred to UTC(CH) for all epochs without interpolation and the TAI link calibration no longer depends on the virtual synchronization between paper and hardware clocks [1]. The hardware definition of UTC(CH) is chosen from one of two independent master clocks: UTC(CH.A) and UTC(CH.B). Each is the output from a DDS (Direct Digital Synthesis) synthesizer, used as a

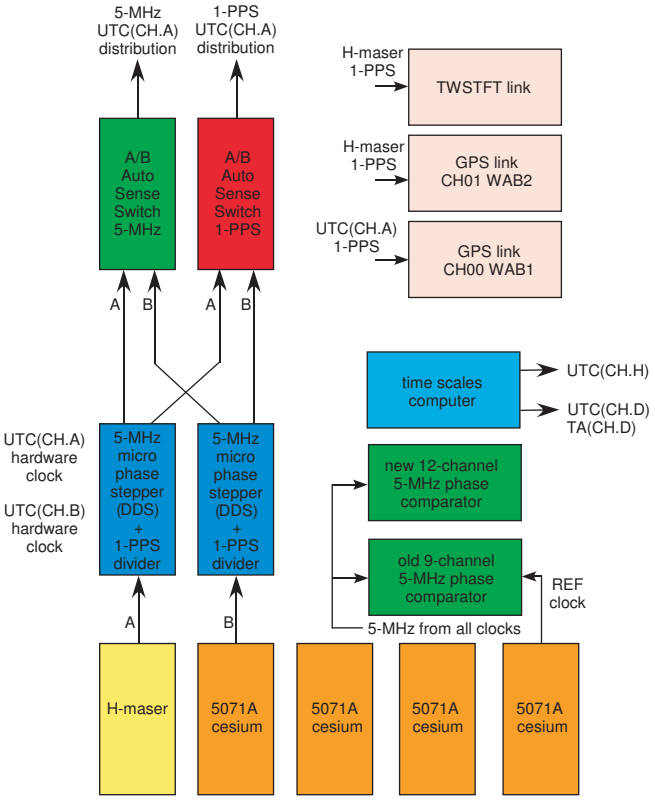

Fig. 1. New time scale generation scheme: UTC(CH) is defined as main master clock UTC(CH.A) or alternate master clock UTC(CH.B).

Micro-Phase Stepper (MPS). Auto-sense Fault Switches (AFS) are used to choose which master clock defines UTC(CH). The hardware redundancy between UTC(CH.A) and UTC(CH.B) has two advantages. One is reliability: if one master clock fails, switching to the alternate master clock is instantaneous. The second is availability: if maintenance becomes necessary on one master clock it is possible to switch to the alternate master clock at one's convenience without interruption of service. The advantages of a paper clock definition are preserved with the new scheme since the master clocks inherit the high stability of a reference computed time scale via the steering process. Moreover, the daily clock difference data from the five clocks

1-4244-0647-1/07/$20.00 ©2007 IEEE

and the TA(CH.D) data that are sent to BIPM at the end of each month are referred to the master clock definition of UTC(CH) and no longer to the computed time scale.

III. Time Scale Generation Method

The main time scales are named UTC(CH.D) and TA(CH.D). Both are computed daily for epoch UTC 00:00 on the basis of phase difference measurements made on five free running atomic clocks: a hydrogen maser and four cesium clocks. The "D" in "CH.D" stands for *Daily*. TA(CH.D) is a free running time scale while UTC(CH.D) is steered monthly to track UTC using a predictive method [4]. The steering of UTC(CH.D) is actually performed by adding a constant to each of the rate state variables of the five clocks. Since the time scale algorithm is based on clock differences, it is impervious to any rate component that is common to all the clocks, so the effect of a steering is visible only with respect to UTC and does not induce a transient in the internal time scale generation process. The time scale generation process is based on the original NBS algorithm [5] . Each day at UTC 00:00, the new clock states are updated using the fundamental time scale equation, [6]

$$x_i(t+\tau) = \sum_{j=1}^{n} w_j(t)\left[\hat{x}_j(t+\tau) - x_{ji}(t+\tau)\right], \qquad (1)$$

where $x_i(t+\tau)$ is the new state of clock i for the current day, the $w_j(t)$ are the clock weights of the previous day, the $\hat{x}_j(t+\tau)$ are the predicted clock states for the current day, the $x_{ji}(t+\tau)$ are the measured clock differences for the current day at UTC 00:00, referred to clock i and n is the total number of clocks in the ensemble. Since we have only five clocks altogether, we had to put the hydrogen maser in the same clock ensemble as the cesium clocks. However the original NBS algorithm was not designed to handle a drifting clock. If nothing special is done, the drift of the hydrogen maser drags the time scale into a smaller drift whose magnitude depends on the relative weight of the hydrogen maser with respect to the four cesium clocks. This is a side effect we have experienced ever since the hydrogen maser was introduced in the clock ensemble and that we want to eliminate in the new system. The variant of the NBS algorithm that NIST uses to generate the AT1 time scale [6] solves the problem by introducing a drift correction term in the predictor, [6] equation (1),

$$\hat{x}_i(t+\tau) = x_i(t) + \tau y_i(t,T) + \frac{1}{2}d\tau^2. \qquad (2)$$

We aim to achieve the same result by using a different clock prediction algorithm [7]

$$\hat{x}_i(t+\tau) = x_i(t) + \tau y_i(t,T) + \frac{1}{2}d\tau^2\left(1+\frac{T}{\tau}\right) \qquad (3)$$

where $\hat{x}_i(t+\tau)$ is the predicted state of clock i for the current day, $x_i(t)$ is the state of the previous day, τ is the prediction interval *i.e.* one day, $y_i(t,T)$ is the filtered rate of clock i for the previous day, and T is the time constant of the exponential filter used for the rate filtering. The first two terms of the right hand side of equation (3) correspond to the classical linear predictor used when there is no drift. The term $\frac{1}{2}d\tau^2\left(1+\frac{T}{\tau}\right)$ is a bias correction term that takes into account the fact that when one uses the average slope, *i.e.* the average frequency, to predict a parabola, *i.e.* the clock time scale in presence of frequency drift, the systematic error, *i.e.* the bias, on the prediction depends not only on the prediction interval τ but also on the time constant T used for the averaging of the slope. Since for n clocks there are only $n-1$ clock differences, a time scale algorithm based on measured clock differences must be constrained by some additional condition, otherwise the system of $n-1$ equations cannot be solved for n clocks [8]. In the case of the NBS algorithm the implicit condition is

$$\sum_{j=1}^{n} w_j(t)\left[\hat{x}_j(t+\tau) - x_i(t+\tau)\right] = 0. \qquad (4)$$

Equation (4) is a circular condition that stipulates that for every computation epoch the weighted sum of all prediction errors must be zero. Hence if the predictor is biased because it does not model the drift of one of the clocks, then the circular condition propagates the drift to the ensemble. Conversely if the predictor is unbiased, then the time scale is expected to remain free from drift. We have verified by simulations based on real clock measurement data that we can indeed cancel the drift of the time scale by adjusting the drift coefficient in the predictor of the drifting clock.

IV. Master Clock Steering Method

Until recently we used to steer an experimental master clock called UTC(CH.R) using a predictive control algorithm [7] [10]. Since UTC(CH.D) used to be computed every night for UTC 00:00 of the previous day, it was necessary, for the purposes of the daily steering of UTC(CH.R), to predict the state of the reference clock over a time span of 1.5 d. The quality of the steering was limited by the prediction error over this long interval. During the development of the new redundant master clocks UTC(CH.A) and UTC(CH.B) we have radically changed our approach to master clock steering. Instead of predicting the state of the reference clock over a long prediction interval starting with the last computed epoch of UTC(CH.D), we generate an extended time scale, called UTC(CH.H) which is computed every hour. The "H" in "CH.H" stands for *Hourly*. This time scale can be seen as an extension of the main time scale between the last computed epoch of UTC(CH.D) and the current epoch. The computation of UTC(CH.H) starts with the last computed state variables of UTC(CH.D) which are used as the initial conditions. Next, the clock difference measurements are used to compute UTC(CH.H) for every integer hour starting with the epoch of the last UTC(CH.D) computation, up to the present epoch. The steering of the master clock is performed at every integer hour, right after the computation of the extended time scale. Hence, a prediction is not necessary to know the state of the master clock at the epoch of the current steering. However, the steering control algorithm is still predictive in the sense that the computed DDS rate command is designed

to cancel the master clock error predicted for the epoch of the next steering. There are both, a frequency correction term y_1 and a phase correction term y_2 in the rate correction command Δy that is programmed into the DDS at the current epoch t,

$$\Delta y(t) = y_1(t) + y_2(t). \tag{5}$$

The terms of (5) are

$$y_1(t) = -y_r(t, T) \tag{6}$$

and

$$y_2(t) = -\hat{x}_s(t + \tau)/\tau = -x_s(t)/\tau. \tag{7}$$

The instantaneous output rate of the master clock is $y_m(t) = y_r(t) + \Delta y(t)$ whereas $y_r(t, T)$ is the filtered rate of the free running reference clock that drives the DDS. Hence, the purpose of the frequency correction term (6) is to cancel the average rate of the steered master clock with respect to the extended time scale UTC(CH.H). On the other hand the purpose of the phase correction term (7) is to cancel the predicted master clock time error within a single steering interval τ. Note that since the average rate of the master clock is zero thanks to the frequency correction term, the predicted master clock time error $\hat{x}_s(t + \tau)$ is identical to the current time error $x_s(t)$. The steering algorithm is actually the same as that used previously to steer UTC(CH.R) [10]. The only difference is that with the use of the extended time scale, the prediction interval can be reduced to one hour. Such a steering algorithm, that tries to cancel the time error within a single steering interval, is not optimal in the sense of minimizing the residual white phase noise. However, the algorithm is robust in the sense that it can recover very quickly, actually within a single steering period, from any perturbation of the reference clock. It is clearly not optimal to use the state variables of a daily time scale as the initial conditions to compute an hourly time scale. As a matter of fact, the extended time scale is always in a transient. It starts with parameters optimal for a one day sampling interval and then, hour after hour, the adaptive algorithm tries to optimize the time scale parameters for a one hour sampling interval. But after 24 hours, before steady state is reached, the time scale is reset with new initial conditions. Nevertheless, this approach is very convenient because it offers both the advantages of an hourly time scale (the master clocks can be steered every hour and the prediction interval in the steering algorithm is only one hour) and the advantages of a daily time scale (if something goes wrong with the atomic clocks or with the measurement and control hardware, we have 24 hours to fix the problem without affecting the main time scale). We have verified that over the 24 hour maximum time interval over which the extended time scale is integrated, the divergence between the hourly and the daily time scale is negligible. Figure 2 shows the difference between the hourly state of hydrogen maser C5 (continuous line) *vs* UTC(CH.H) and the daily state (squares) *vs* UTC(CH.D) of the latter when the extended time scale is integrated exceptionally over several days without a reset. For epoch 0 the initial conditions are the same and both time scales

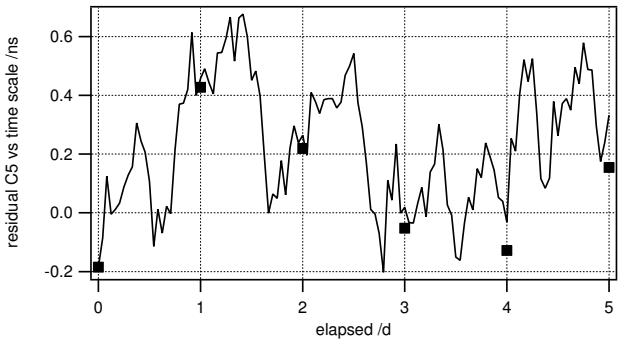

Fig. 2. Difference between the extended time scale UTC(CH.H) (line) and the main time scale UTC(CH.D) (squares), referred to hydrogen maser clock C5, when the extended time scale is exceptionally integrated over several days. After 4 days of integration the discrepancy between the time scales is only 0.1 ns.

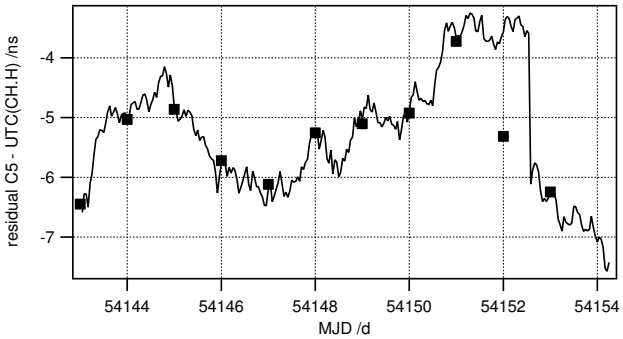

Fig. 3. Difference between the extended time scale UTC(CH.H) (line) and the main time scale UTC(CH.D) (squares) referred to hydrogen maser clock C5 in normal operation. A steering of UTC(CH.D) occurs at epoch MJD 54151 UTC 00:00.

are identical. After one day of integration, the divergence is still negligible. After 4 days of integration the discrepancy between the extended and the main time scales reaches about 0.1 ns, which is small enough to consider the two time scales as practically identical. Figure 3 shows the difference between the hourly state versus UTC(CH.H) (continuous line) and the daily state versus UTC(CH.D) (squares) of hydrogen maser clock C5, in normal operation when the extended time scale UTC(CH.H) is reset at every new computation of UTC(CH.D). Note that on MJD 54252 it was decided, after the fact, to apply manually a rate correction to UTC(CH.D) effective at epoch UTC 00:00 of MJD 54151. Now observe that, at UTC 00:00 on MJD 54152, UTC(CH.H) was still tracking the original, un-steered, UTC(CH.D) because the state variables had not yet been modified to apply the steering rate correction. Hence the temporarily discrepancy (1 ns) between the extended time scale and the modified (steered) main time scale. Then, in the middle of MJD 54152, the UTC(CH.D) state variables were updated and at the next steering epoch, UTC(CH.H) suddenly made a jump to track the modified (steered) UTC(CH.D). Figure 4 shows the difference between the hourly state *vs* UTC(CH.H) (continuous line) and the daily

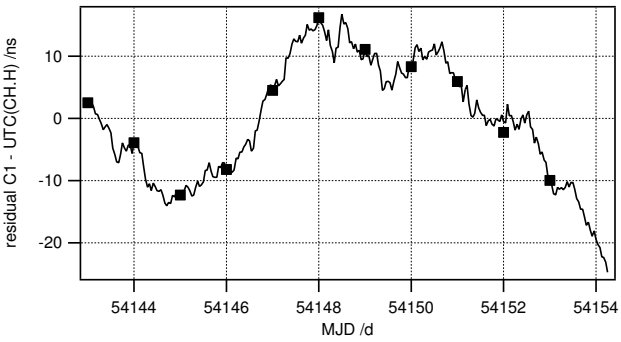

Fig. 4. Difference between the extended time scale UTC(CH.H) (line) and the main time scale UTC(CH.D) (squares) referred to cesium clock C1 in normal operation. A steering of UTC(CH.D) occurs at epoch MJD 54151 UTC 00:00.

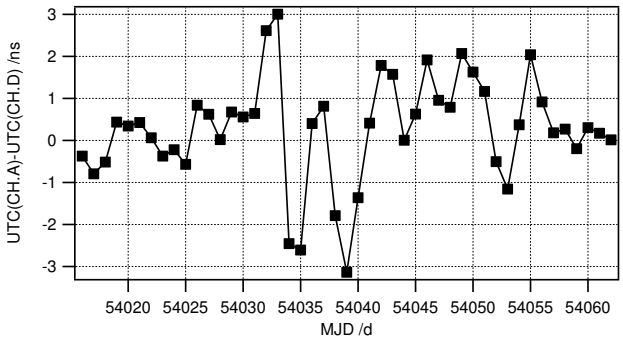

Fig. 5. Time process UTC(CH.A)-UTC(CH.D) observed from MJD 53157 to MJD 53438. Master clock A is driven by a hydrogen maser. The steering is performed once a day and the prediction interval is 1.5 d. The distribution is gaussian and the standard deviation is 1.4 ns.

state *vs* UTC(CH.D) (squares) of clock C1, a cesium clock, in normal operation, recorded during the same period. We observe that in the case of the cesium clock the 1 ns jump due to the retroactive steering of UTC(CH.D) is masked by the random fluctuations of the cesium clock.

V. Past and Present Master Clock Results

Up to April 2002, a cesium clock and a conventional feedback control algorithm were used to generate UTC(CH.R) [9]. The RMS deviation of the difference UTC(CH.R)-UTC(CH.D) was about 8 ns. Then from April 2002 to May 2004 we used a first version of a predictive control algorithm without much improvement over the original feedback algorithm [10]. In May 2004 we started using a hydrogen maser and an improved predictive control algorithm to generate UTC(CH.R) [7] [11]. With the improved algorithm the RMS deviation was reduced to 1.4 ns *i.e.* an order of magnitude improvement with respect to the previous UTC(CH.R) generation scheme. Then in 2006 we started to generate the master clocks A and B driven respectively by a hydrogen maser and a cesium clock. Figure 5 shows the time process UTC(CH.A)-UTC(CH.D) steered directly to UTC(CH.D) with a 1 d steering interval and 1.5 d prediction interval. The standard deviation is 1.4 ns. Figure 6 shows the time process UTC(CH.B)-UTC(CH.D) steered directly to UTC(CH.D) with a 1 d steering interval and 1.5 d prediction interval. The standard deviation is 3 ns.

The results reviewed above are to be compared with the current performance of the master clocks UTC(CH.A) and UTC(CH.B) that we obtain using the extended time scale and a one hour prediction interval. Figure 7 shows the time process UTC(CH.A)-UTC(CH.H). Master clock A is driven by a hydrogen maser. The steering is performed at the beginning of each hour to track the extended time scale UTC(CH.H). The measured standard deviation is 0.2 ns *i.e.* a seven fold improvement with respect to the previous scheme driven by the same hydrogen maser. The improvement stems from the use of the extended time scale. Figure 8 shows the time process UTC(CH.B)-UTC(CH.H). Master clock B is driven by a cesium clock. The standard deviation is 0.5 ns which is

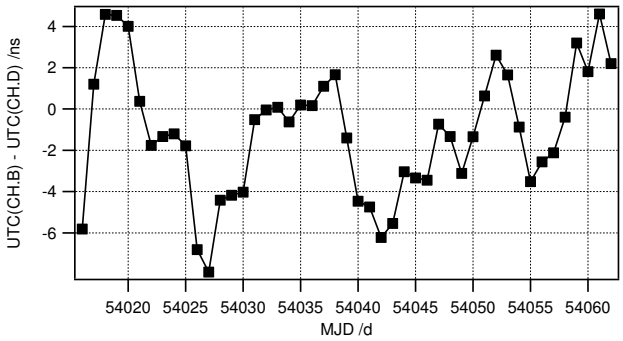

Fig. 6. Time process UTC(CH.B)-UTC(CH.D) observed from MJD 53157 to MJD 53438. Master clock B is driven by a cesium standard. The steering is performed once a day and the prediction interval is 1.5 d. The distribution is gaussian and the standard deviation is 3 ns.

not as good as the 0.2 ns of master clock A. The differences UTC(CH.A)-UTC(CH.H) and UTC(CH.B)-UTC(CH.H) are both white noise processes. This behavior comes from the fact that the predictive steering control algorithm tries to cancel the predicted master clock error within a single steering interval. What happens during the current steering interval is uncorrelated with what happens during the previous or next steering intervals. The Allan deviation of master clock A is $\sigma_y(\tau) = 2.5 \times 10^{-10}\tau^{-1}$ while the Allan deviation of master clock B is $\sigma_y(\tau) = 6.3 \times 10^{-10}\tau^{-1}$. Figure 9 shows the residual of UTC(CH.A) *vs* the free running hydrogen maser C5. The residual is the master clock state *vs* C5 phase translated to a zero initial state and frequency translated to a zero average rate. The master clock A is extremely stable on the short-term because it is driven by a hydrogen maser. This is why we observe that the dominant source of time fluctuations is the control algorithm itself. Rate corrections of alternate signs are made at the beginning of every hour, in an attempt to cancel the prediction error, hence the triangular waveform. On the other hand Figure 10 shows the residual of UTC(CH.B) *vs* the free running hydrogen maser C5. It can be observed that the short-term stability of master clock B is not as good as that of master clock A, hence the action of the control

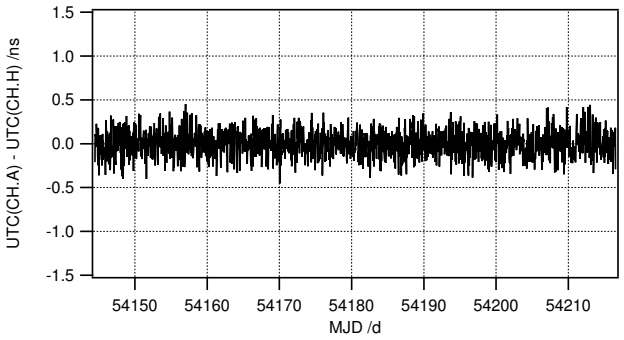

Fig. 7. Time process UTC(CH.A)-UTC(CH.H) observed from MJD 54144 to MJD 54217. Master clock A is driven by a hydrogen maser. The steering is performed once an hour.The distribution is gaussian and the standard deviation is 0.2 ns.

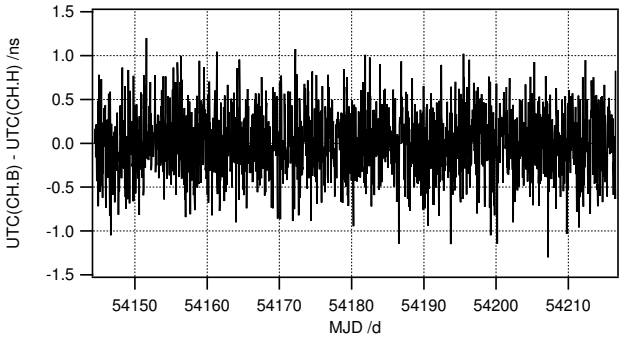

Fig. 8. Time process UTC(CH.B)-UTC(CH.H) observed from MJD 54144 to MJD 54217. Master clock B is driven by a cesium clock. The steering is performed once an hour. The distribution is gaussian and the standard deviation is 0.5 ns.

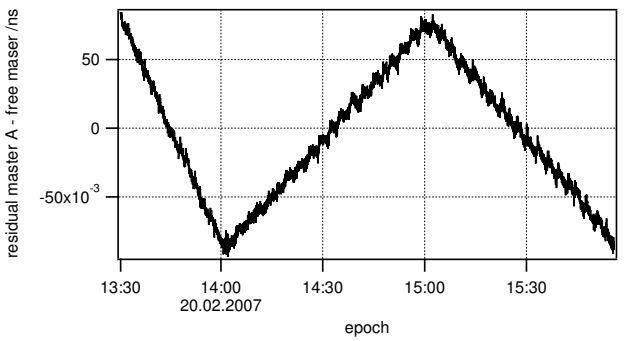

Fig. 9. Residual of UTC(CH.A) *vs* free running hydrogen maser C5. The dominant source of time fluctuations is the control algorithm itself. Rate corrections of alternate signs are made at the beginning of every hour, in an attempt to cancel the prediction error, hence the triangular waveform.

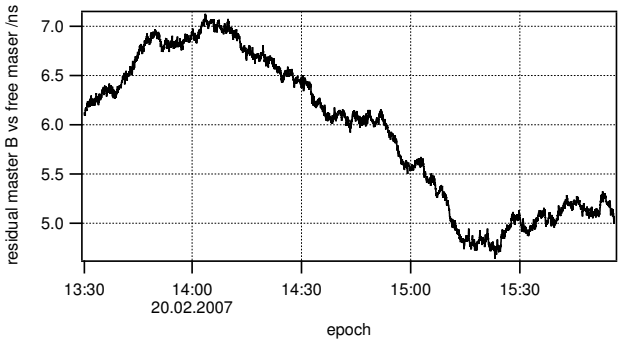

Fig. 10. Residual of UTC(CH.B) *vs* free running hydrogen maser C5. The short-term stability of master clock B is not as good as that of master clock A, hence the action of the control algorithm is not as conspicuous.

algorithm is not as conspicuous as it is in the previous case. In conclusion, it is clear that the master clock steering method that we have chosen does not take full advantage of the short-term stability of the hydrogen maser. Behind that decision is the fact that we have only one hydrogen maser. If master clock A were optimized to fully exploit the short-term stability of the hydrogen maser, we would have a dramatic degradation of performance every time we switch to master clock B. Instead, we prefer to rely on a master clock defined UTC(CH) with constant frequency stability characteristics. However, we keep the possibility to use the free-running hydrogen maser as the reference clock to drive any system that requires an excellent short-term frequency stability, for example the WAB2 IGS station and the TWSTFT link.

VI. Time Scale Generation and Control Issues

Figure 11 shows the history of UTC(CH) *vs* UTC as recorded in the BIPM data base. The obvious feature of this figure is the dramatic improvement of stability that occurred after August 2001 (MJD 53143) when a predictive steering algorithm was first applied to UTC(CH.D) [9]. However, it can also be observed that, after August 2001, there is a succession of quiet intervals, during which the predictive steering algorithm is able to track UTC very closely, separated by disturbances. The latter are usually produced by accidental rate steps of the clocks, which are difficult to calibrate and compensate when only a few clocks are available [4]. More rarely, the disturbances are the consequence of glitches in the clock difference measurement process. Indeed, if there is a shortage of clock measurement data, following a glitch in the data acquisition process, the time scale generation process is disrupted. Once there is a gap in the data set, the only way to go on with the time scale generation process is to interpolate the clock difference data. Such a disruption of the time scale generation process has two side effects. One effect is a rate step of the time scale. The other effect is a loss of calibration of the TAI link which, in the context of a paper time scale definition of UTC(CH), is partially founded on the continuity of the time scale generation process [1]. The longer the data shortage, the more severe the side effects. In the new system we address these issues in two different ways. On the one hand we have already improved the robustness of the clock data acquisition process by introducing hardware redundancy in the phase measurement system [1]. On the other hand the TAI link "paper" calibration loss issue is one of the main motivations for the change of UTC(CH) definition since "paper" calibration problems vanish in the context of a

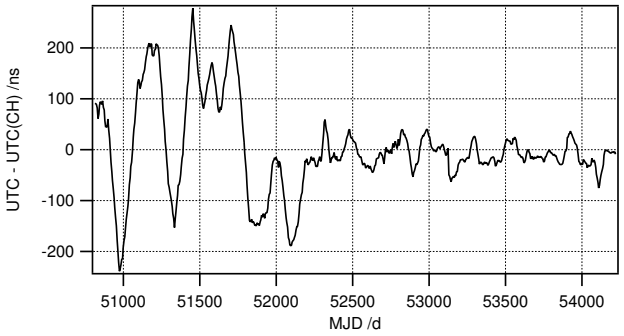

Fig. 11. UTC - UTC(CH) historical data as found in BIPM data base. A dramatic improvement of the stability occurred in August 2001 (MJD 53143) after we started to use a predictive steering control algorithm.

"hardware" definition of UTC(CH).

VII. TAI Link and Master Clock Calibration

We are currently in the validation phase, working with a hybrid system in which the old definition of UTC(CH) is still applied although the new master clock architecture is ready. Moreover, the TAI link is still driven by the 1-PPS signal from a reference cesium clock. As reported above, the extended time scale UTC(CH.H) and the main time scale UTC(CH.D) can be considered identical. In this transitional configuration, we calibrate the master clocks A and B by comparing their 1-PPS signals with the 1-PPS signal from the reference cesium clock [1]. A time interval counter measurement of the 1-PPS signal from the master clocks A and B versus the reference 1-PPS signal from the reference cesium clock, and the knowledge of the state difference REF-UTC(CH.D) yields the initial values of the states UTC(CH.A)-UTC(CH.D) and UTC(CH.B)-UTC(CH.D) that must be written into the state variables to establish consistency between the paper clocks and the 1-PPS hardware states of the master clocks. The TAI link calibration is such that when the 1-PPS signal of the reference cesium clock is compared with the pivot laboratory UTC(k) via the TAI GPS link, the result is consistent with the state of REF-UTC(CH.D) and with the state UTC(CH)-UTC(k) published in *Circular T*. This means that the TAI link calibration applies to a hybrid system of "hardware" and "paper" internal delays. The "paper" internal delays remain constant only as long as the time scale generation process is not disrupted [1]. Hence the risk of losing calibration in case of a data acquisition glitch as mentioned in the previous section. When the validation phase is over, the TAI link will be driven either by the 1-PPS signal from the master clock itself or by the 1-PPS signal from one of the free running clocks. In either case, calibration will be simpler than it is now, since the master clock 1-PPS output will be the definition of UTC(CH). There will be no more "paper" internal delays in the part of the system covered by the TAI link calibration, hence no risk of calibration loss, and a time interval counter measurement of the 1-PPS signal from any clock that drives the TAI link *vs* the 1-PPS signal from the master clock will be sufficient to get a consistent system calibration.

VIII. Conclusions

The experimental results reported in this paper are representative of what will be the actual performance of the new master clock definition of UTC(CH) once the new system has been commissioned. Since master clock A is able to track the paper time scale with a 0.2 ns accuracy, whereby UTC(CH.D) fluctuates from month to month by several ns, the change from a "paper" to a "hardware" definition of UTC(CH) is expected to bring its advantages without degrading the current stability of UTC(CH). The stability of the main time scale UTC(CH.D) is currently and will remain limited by the number and by the frequency stability of the clocks in the ensemble. With a master clock definition of UTC(CH) the TAI link calibration will be free of "paper" delays. Moreover, the improved time scale algorithm is expected to eliminate the small drift that currently affects UTC(CH.D) and TA(CH.D). The main progress achieved recently was a large improvement of the tracking performance of the master clocks *vs* the "paper" time scale. In the case of master clock A the RMS deviation was reduced from 1.4 ns down to 0.2 ns. In the case of master clock B the RMS deviation was reduced from 3 ns down to 0.5 ns. As discussed above, the steering control parameters do not take full advantage of the short-term stability of the hydrogen maser. The reason is that we have only one hydrogen maser whereas we need a pair of redundant master clocks with equivalent frequency stability characteristics. However, we will continue to use the free-running hydrogen maser as the reference clock to drive applications that requires an excellent short-term frequency stability such as the WAB2 IGS station and the TWSTFT link. We plan to commission the new definition of UTC(CH) before the end of 2007.

References

[1] L. G. Bernier, G. Dudle, C. Schlunegger, "METAS New Time Generation System: A Progress Report" *Proc.* 38^{th} *PTTI*, 5-7 December 2006, Reston, VA, USA.

[2] D. Matsakis, "Time and Frequency Activities at the US Naval Observatory", *Proc. Joint IEEE IFCS &* 37^{th} *PTTI*, 29-31 August 2005, Vancouver, BC, Canada, pp.217-224.

[3] Y. Hanado, K. Imamura, M. Imae, "Upgrading of UTC(CRL)", *Proc. Joint IEEE IFCS &* 17^{th} *EFTF*, 4-8 May 2003, Tampa, FL, USA, pp.296-300.

[4] L. G. Bernier, "A Prediction Method Applicable to Steered Time Scales", *Proc. EFTF 2005*, Besançon, France, March 2005, pp.74-78.

[5] D. W. Allan, J. E. Gray, H. E. Machlan, "The National Bureau of Standards Atomic Time Scale: Generation, Stability, Accuracy and Accessibility", in *Time and Frequency: Theory and Fundamentals*, B. E. Blair, Editor, NBS Monograph 140, May 1974.

[6] M. Weiss, T. Weissert, "AT2, A New Time Scale Algorithm: AT1 Plus Frequency Variance", *Metrologia*, vol. 28, 1991, pp. 65-74.

[7] L. G. Bernier, "Predictability of a Hydrogen Maser Time Scale", *Proc. EFTF 2005*, Besançon, France, March 2005, pp. 438-441.

[8] S. R. Stein, "Time Scales Demystified", *Proc. Joint 2003 IEEE IFCS and* 17^{th} *EFTF*, Tampa, FL, 5-8 May 2003, pp.223-227.

[9] L. G. Bernier, "Experimentation at METAS with a Simple Steering Algorithm based on Linear Prediction", *Proc.* IV^{th} *International Time Scale Algorithms Symposium*, BIPM, Sèvres, France, March 18-19 2002.

[10] L. G. Bernier, G. Dudle, "Practical Performance of the UTC(CH.R) Real Time Realization of UTC(CH) and Prospects for Improvement", *Proc. EFTF 2004*, University of Surrey, Guildford, UK, April 5-7 2004.

[11] L. G. Bernier, "METAS Time & Frequency Metrology Report", *Proc. 2005 Joint IEEE IFCS and PTTI*, Vancouver, Canada, August 2005.